

Chapter 5

Phase Diagram Involving the Twist Grain Boundary Phase in the Vicinity of a Virtual Cholesteric-Srnectic A-Smectic C* Point

5.1 Introduction

The nature of the nematic - smectic A - smectic C (NAC) meeting point has been the subject of extensive experimental studies[1,2]. These studies have been made all the more interesting by the recent predictions[3,4,5] of the chiral version of the Chen-Lubensky(CL) model[6]. Depending on the strength of chirality, this theory expects different topologies for the meeting point. When the chirality is zero one gets the usual NAC - multicritical point. In the presence of a chiral field the theory proposes two alternatives depending on whether the system behaves like a type I or type II superconductor. In the case of the former, the chiral nematic (cholesteric or Ch), smectic A (A) and chiral smectic C (C*) phases meet at a critical end point. In type II systems the meeting point is preempted by the appearance of a new type of phase, namely, the *Twist Grain Boundary* (TGB) phase[3] which is the liquid crystal analogue of the Abrikosov flux lattice in superconductors[7]. On the experimental side, the zero chirality case - the NAC multicritical point - is well established[1,2,8]. For the chiral version, two different types of meeting point, viz., a triple point[9] and a multicritical point[10] have been reported. However, the TGB phase, recognised to be identical[11] to the A* phase discovered by Goodby et al[12], has not been found near the Ch-A-C* meeting point. This chapter describes the observation of a phase diagram in which the TGB phase appears, as expected by the theory, near a virtual Ch-A-C* meeting point.

5.1.1 Analogy between the Normal-Superconductor and the N-A transitions

The basis of the analogy between the normal-superconducting transition in metals and the nematic-smectic A (N-A) transition in liquid crystals is that the ordered phases of both smectic A and superconductors are characterised by a non-vanishing complex order parameter ψ [13]. For a superconductor the order parameter is the wave function whereas for the smectic A phase it is the mass density wave. The coupling between the smectic order parameter and the director fluctuation δn is similar to that between the superconductor order parameter and the vector potential A . Furthermore, the spatial average of the twist $n \cdot (\nabla \times n)$ corresponds to the magnetic induction B . The field h conjugate to the twist, corresponds to the magnetic intensity H . Thus, the cholesteric phase is the analogue of a normal metal in an external magnetic field. The expulsion of twist occurring at the cholesteric to smectic A transition is then the liquid crystal analogue of the Meissner effect.

Renn and Lubensky extended [3] these arguments to find the analogue of the Abrikosov flux lattice phase in liquid crystals containing chiral molecules. Superconductors have been classified into type I and type II depending upon the value of the Ginzburg parameter $k \equiv \lambda/\xi$, where λ is the penetration depth (the thickness over which a deformation, for e.g., a weak magnetic field, penetrates the surface of the normal metal) and ξ is the coherence length (the distance over which the local perturbation affects the amplitude of ψ). For type I superconductors, $k < \frac{1}{\sqrt{2}}$ and for type II, $k > \frac{1}{\sqrt{2}}$. If the material is a type

In a type I superconductor then below the critical temperature the field lines of the applied magnetic field are completely expelled. This is the Meissner effect. On the other hand a type II superconductor exhibits a phase intermediate between the normal and superconducting phases, in which the magnetic field lines form a triangular array of vortices. The lattice of vortices is known as the Abrikosov flux lattice[7]. The triangular lattices of vortices and the structure of a vortex line is shown in Figure 5.1. In type-I systems, fluctuations drive the second order mean-field normal to superconducting transition first order[14]. If the N-A transition behaves like a type I transition then it would always be first order and there would be no flux lattice analogue. In type II systems fluctuations are believed to lead to a second order transition characterised by the inverted XY model behaviour[15]. Although theoretical studies indicated that N-A transition belongs to an inverted XY class, experiments have shown XY class behaviour for a number of materials[16]. As such one can expect to observe the liquid crystal analogue of the Abrikosov phase.

Renn and Lubensky have argued that this phase can be realised when the chiral molecules are present in the system and would consist of a regular array of parallel twist grain boundaries composed of regularly spaced parallel twist dislocations with axes that rotate from one grain boundary to the next and termed it as the *Twist Grain Boundary* (TGB) state. The schematic representation of the cholesteric(Ch) phase and the TGB phase with its pitch axis parallel to the X axis are shown in Figure 5.2. In the case of Ch phase the director \hat{n} lies the YZ plane and rotates in a helical fashion as the coordinate X along the pitch axis increases. The average configuration of the director in TGB phase is very

Chapter 5: Phase diagram involving the TGB phase..

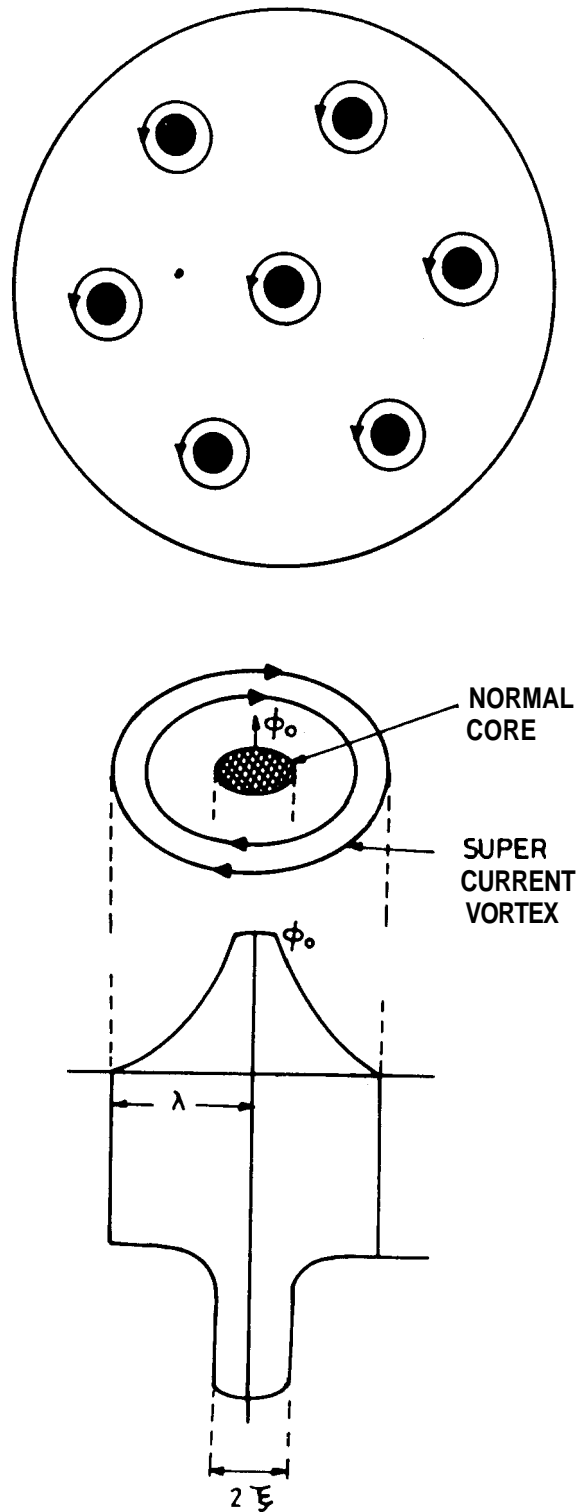


Figure 5.1: (a) The triangular lattices of vortices. (b) Structure of a vortex line. (From A. V. Narliker and S. N. Ekbote, *Superconductivity and superconducting materials*, p.43 (1983)).

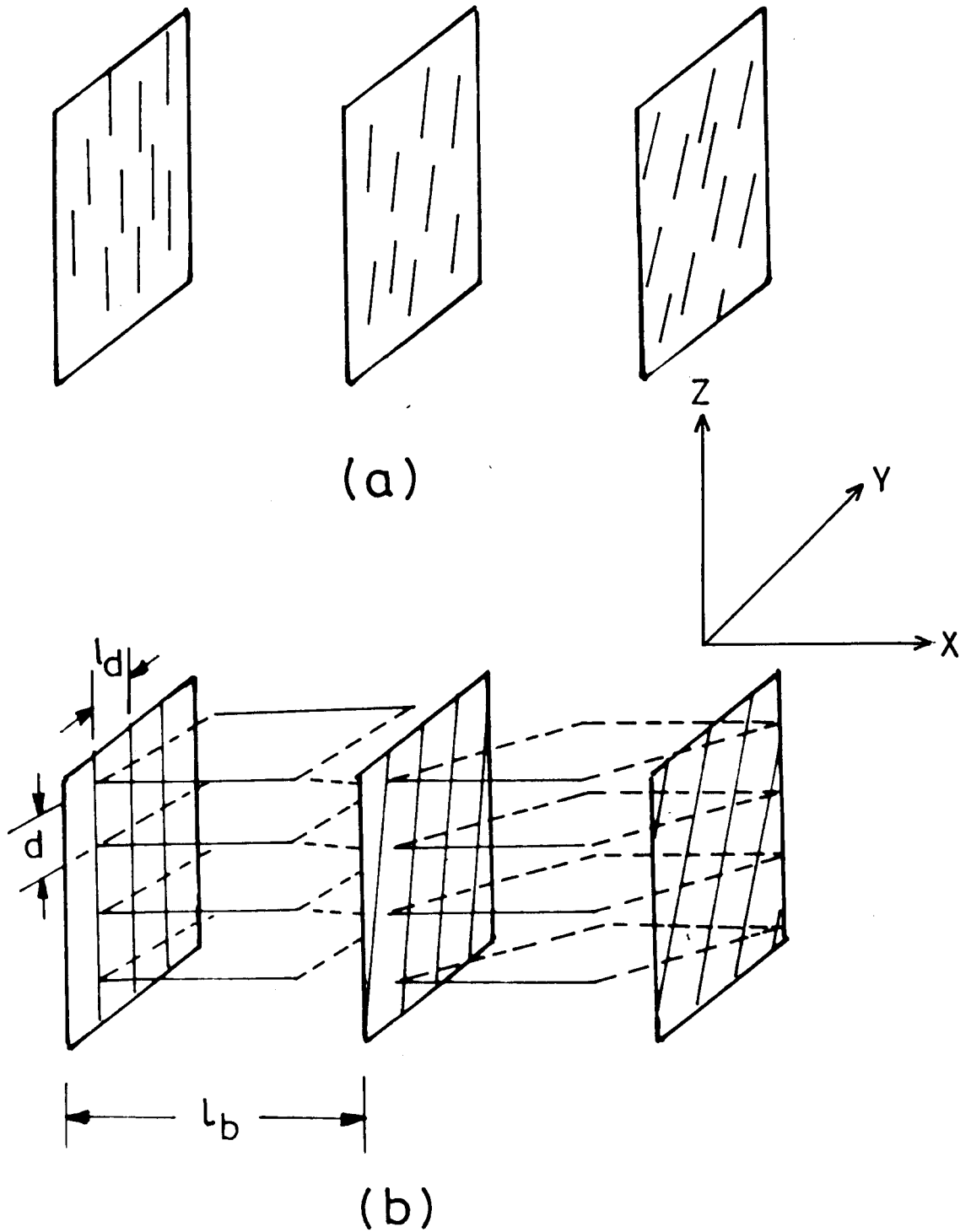
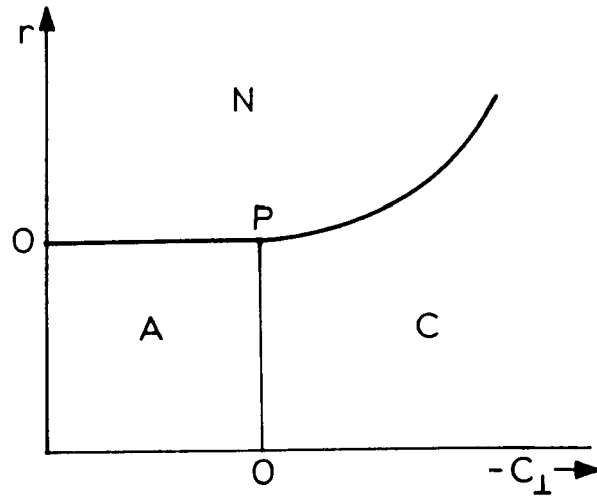


Figure 5.2: (a) Schematic representation of a cholesteric(Ch) liquid crystal. (b) Schematic representation of the TGB state.(from Ref.[4])

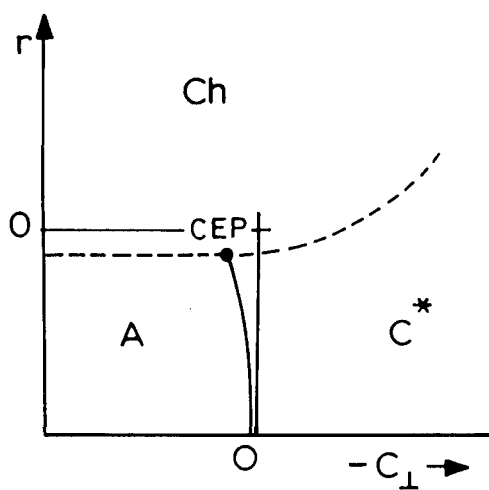
similar to that of the Cl phase. For the TGB state, there are regularly spaced twist grain boundaries separated by a distance l_b . Each grain boundary consists of regularly spaced screw dislocations separated by a distance l_d . The configuration of molecules between the grain boundaries is essentially identical to that of the A phase with regularly spaced layers separated by a distance d .

5.1.2 Chiral Chen-Lubensky(CL) Model

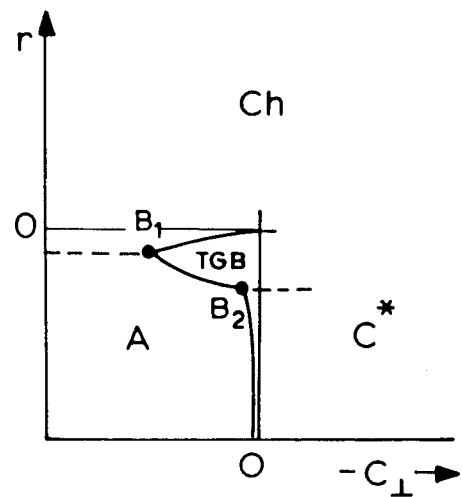
A phenomenological model introduced by Chen and Lubensky[6] has been very successful in explaining experimental observations in the vicinity of the NAC multicritical point. Lubensky and Renn have generalised[4,5] this model to describe the effects of chirality on the NAC point and its immediate neighbourhood. One essential feature of these models is that the C phase is induced by the tilt of the nematic director relative to the layer normal. The sign of the coefficient of the transverse gradient term C_{\perp} decides whether the ordered phase is A or C phase. In the latter model in addition to the reduced temperature $r \sim T - T_{NA}$ (where T_{NA} is the N-A transition temperature) and the coefficient C_{\perp} used in the NAC model, the chiral field h is introduced as one more variable. When $h=0$, the phase diagram in the $C_{\perp} - r$ plane, reduces to the original NAC diagram (Figure 5.3(a)). Notice that all the phase boundaries NA, NC and AC are second order at the meeting point(P) and thus it is a multicritical point. When $h \neq 0$ there are two possibilities depending upon whether the system behaves like a type I or type II superconductor. If the material is type I the Cl-A and Cl-C* transitions would be first order whereas the A-C* transition is second order and terminates at a critical end point CEP(See Figure 5.3(b)). More in-



(a)



(b)



(c)

Figure 5.3: (a) Mean-field phase diagram for the Chiral CL model in the r - C_{\perp} plane when $h=0$. P is the NAC multicritical point. (b) Mean-field phase diagram for the chiral CL model when $h \neq 0$ for type I systems. The dashed line is the first order boundary and the solid line second order. The A- C^* transition line terminates at a critical end point (CEP). (c) Mean-field phase diagram when $h \neq 0$ for type II systems. The TGB phase intervenes between the Ch and A phase. B_1 and B_2 are bicritical points.

interesting things happen when the system is type II. The TGB phase intervenes between C_{li} and A phases as shown in Figure 5.3(c). Both the C_{li}-TGB and TGB-A phase boundaries are second order whereas C_{li}-A would remain first order. Thus the point B₁ at which C_{li}, A and TGB phases meet is a bicritical point. Further analysis[5] of this model brought out more features in this phase diagram viz., appearance of the tilted TGB phase etc. We will not discuss them here.

5.1.3 Experimental background

At around the same time as that of the theoretical prediction[3] of the TGB phase, Goodby et al, reported[12] the discovery of a new liquid crystalline phase, which they termed as A* phase, between the isotropic and the chiral smectic C (C*) phase in some members of the homologous series (S)-1-methylheptyl 4'-[(4'' -n -alkoxyphenyl) propionyloxy-biphenyl-4-carboxylate] (nP1M7). The experimental temperature-alkyl chain length phase diagram for the homologous series nP1M7 is shown in Figure 5.4. The A* phase has properties consistent with its being identified with the theoretically predicted TGB phase. X-ray scattering intensities from unaligned samples of the A* phase are similar to those of a powdered A phase. Experiments using aligned samples showed that the scattering intensity is intense on a cylinder with a symmetry axis coincident with the pitch axis[11] as predicted by the theory for the TGB phase. Also, optical microscopic studies showed cholesteric-like textures for the A* phase[12]. The pitch axis in the A* phase is rotated by 90° with respect to that in the C* phase suggesting that the pitch axis lies in the plane of the layers rather than

Chapter 5: Phase diagram involving the TGB phase...

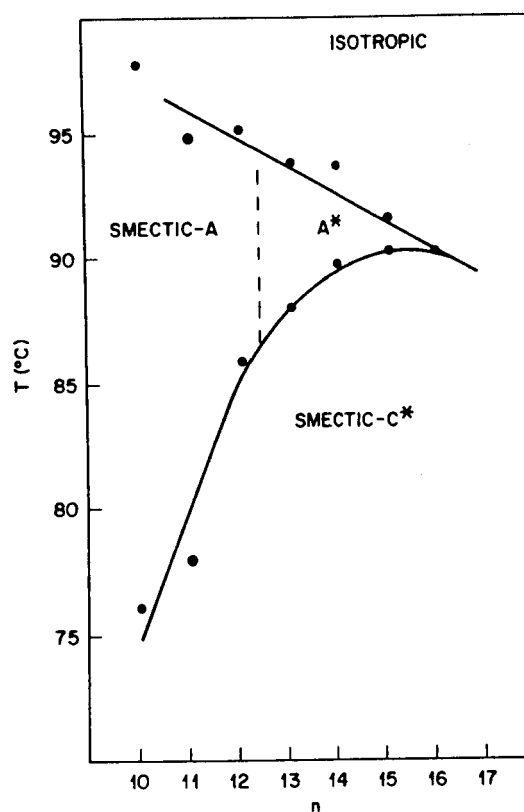


Figure 5.4: Experimental phase diagram for the homologous series $nP1M7$. (from Ref.12).

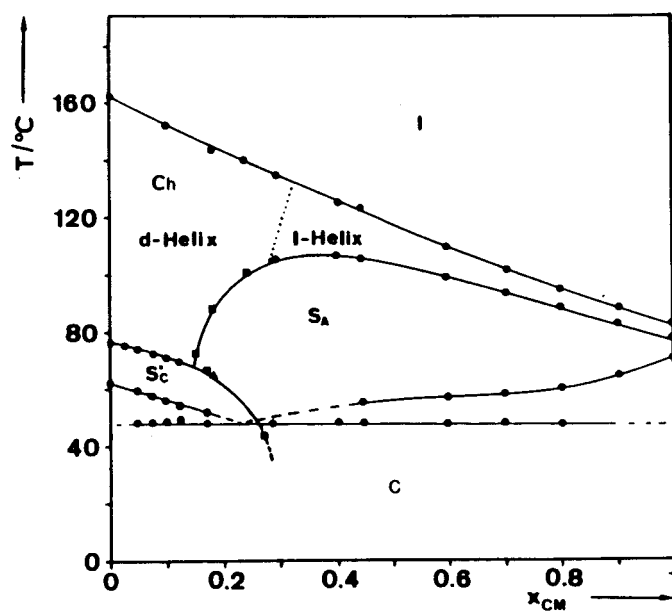


Figure 5.5: Temperature-concentration (T-X) phase diagram of the CE3/CM binary system. The dashed line is the helix inversion line (from Ref.10).

perpendicular to the layers, as in the C* phase. The calorimetry showed clear anomalies[12,17] indicating that the A* and C* phases are indeed distinct thermodynamical phases. Lavrentovici et al, observed in a binary liquid crystalline system, the TGB phase to occur between the Ch and the A phase[18]. Later, Slaney and Goodby found the Ch - A* - A phase sequence to occur in a single component system[19]. Pollmann and Schulte have reported an interesting phase diagram(See Figure 5.5) in which the Ch, A and C* phases meet at a multicritical point and no TGB phase was observed[10]. This could be perhaps due to the following reason. In the vicinity of the multicritical point the sign of the Ch pitch changes giving rise to a helix inversion line (shown as a dashed line in the figure). The large pitch of the Ch phase near the meeting point would reduce the value of the chiral field, thus probably suppressing the TGB phase.

5.2 Experimental

5.2.1 Materials used

Experiments have been carried out on binary mixtures of 4-(2'-methyl butyl) phenyl 4'-n-octyl biphenyl -4-carboxylate(CE8-from BDH) and 4-n-dodecyloxy biphenyl-4'-(2'-methyl butyl)benzoate (C12)[20]. The structural formulae and the transition temperatures of the materials are given in Table 5.1.

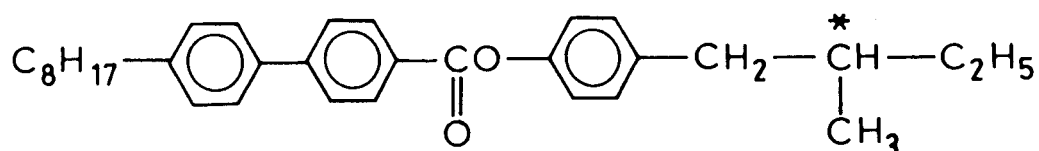
5.2.2 Experimental techniques

To establish the existence of the TGB phase, optical microscopy, DSC, X-ray diffraction and selective reflection techniques have been employed. The DSC

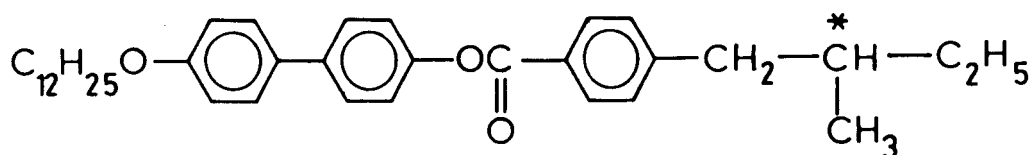
Chapter 5: Phase diagram involving the TGB phase...

Table 5.1: Structural formulae and transition temperatures ($^{\circ}\text{C}$) of the materials used.

CE8



C12



Material	Iso	BP	Ch	A	C*				
CE8	.	139.8	.	135.9	.	134.1	.	84.4	.
C12	.	137.7	.	135.45	.	-	.	117.6	.

Iso= isotropic phase, BP = Blue phase,

Ch = cholesteric, A = smectic A,

C* = chiral smectic C.

and X-ray diffraction methods have been described in the previous chapters. The details of the selective reflection method will be described in 5.3.4.

5.3 Results and Discussion

5.3.1 Optical microscopic studies

The partial temperature concentration (T-X) phase diagram, obtained using a programmable hot stage (Mettler FP82) in conjunction with a polarising microscope, is shown in Figure 5.6. It is seen that for $X < 0.32$ (X is the weight fraction of C12 in CE8) there is a direct Ch-A transition. For $X > 0.32$, a new phase appears which grows at the expense of the A phase and gets bounded near $X = 0.7$. Optical microscopic studies showed that on cooling, the Ch phase transforms into the A phase through an intermediate phase.

The microphotograph obtained for $X = 0.6$ at 118°C is shown in Figure 5.7. The transition to the intermediate phase is signalled by the appearance of the filament texture, characteristic of the TGB phase [12,19]. As the temperature is lowered to the A phase this pattern vanishes resulting in a homeotropic texture. On further cooling the A phase goes to a C^* phase.

For $X > 0.62$, there is no A phase and for mixtures with $0.62 < X < 0.7$ the sequence Ch-TGB- C^* is seen. It is interesting to note that for any concentration the TGB phase occurs at temperatures above the A and/or the C^* phase, a feature observed earlier [19] and also predicted by the theory.

The plane texture (molecular director parallel to the substrate) of the TGB phase shows that it has a helical structure, and the helical axis lies in a direction

Chapter 5: Phase diagram involving the TGB phase...

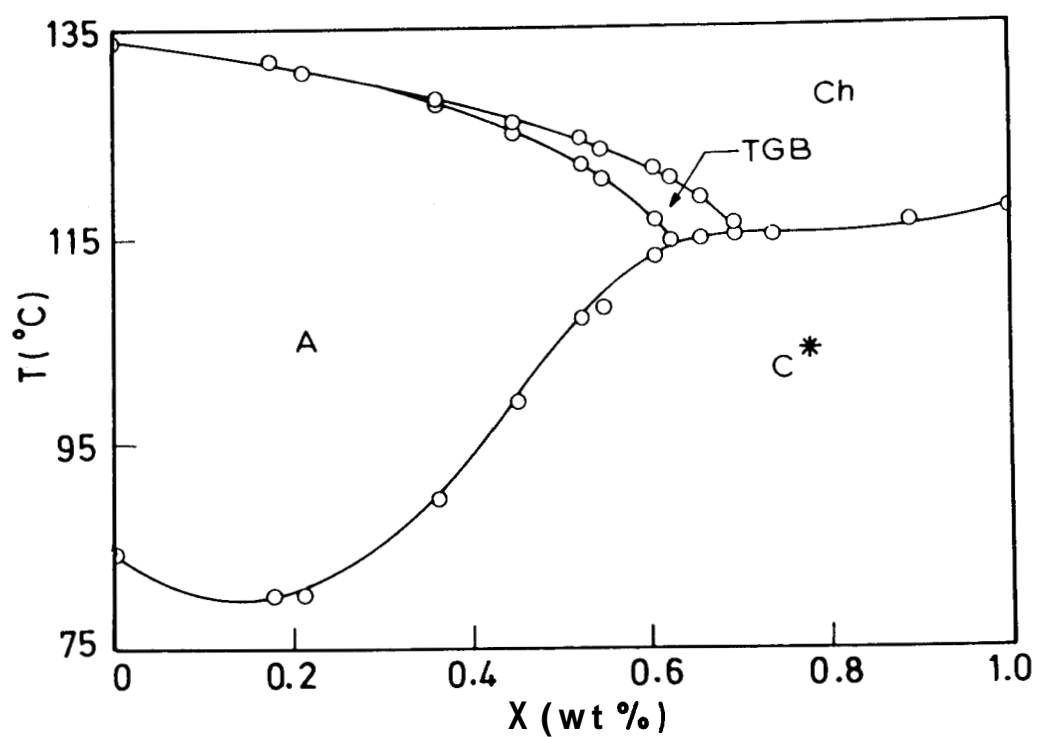


Figure 5.6: Partial temperature-concentration (T-S) diagram for CE8/C12 binary system. X = weight% of C12 in the mixture. The solid lines are meant to serve as a guide to the eye.

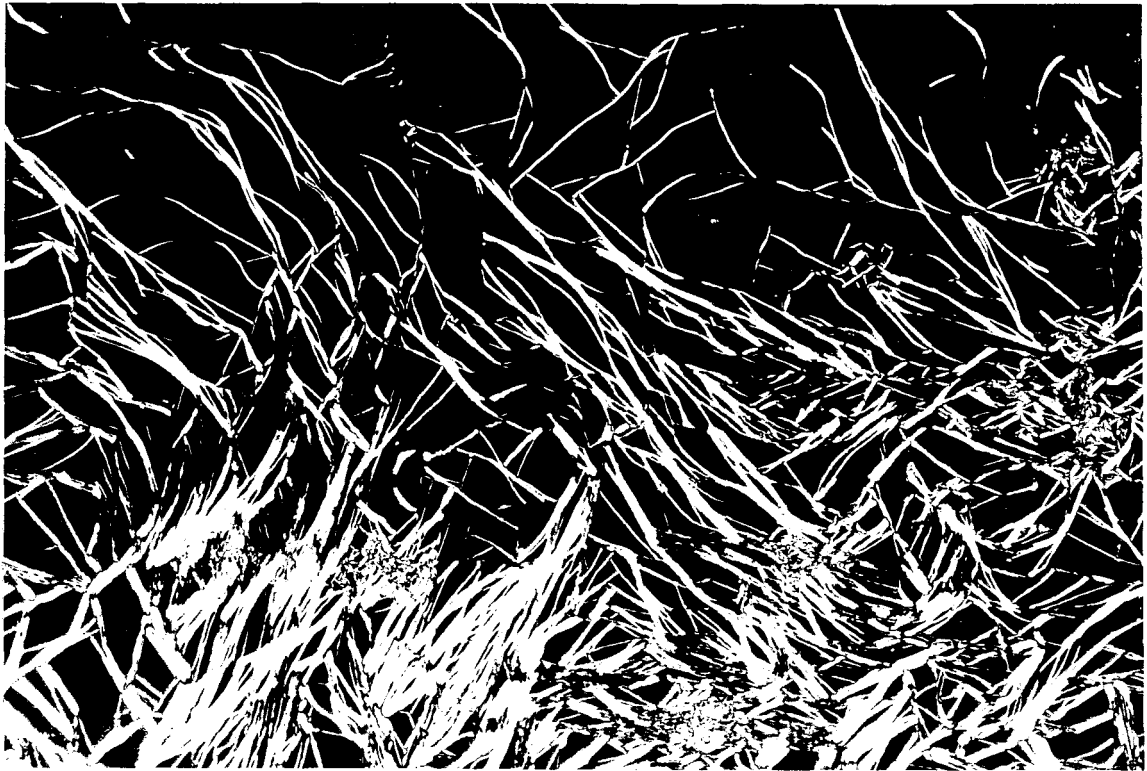


Figure 5.7: The filament texture characteristic of the TGB phase as seen when the sample is cooled from the cholesteric phase. The photograph was taken at $3.6\text{ }^{\circ}\text{C}$ below the Cli-TGB transition point in $X = 0.6$ sample (Magnification: x 125)

parallel to the layers of the phase. Thus, the liquid crystal phase has a twisted layer structure. Selective reflection measurements confirming this structure will be described later.

5.3.2 Differential Scanning Calorimetric (DSC) studies

The differential scanning calorimeter scan for $X = 0.6$ and 0.66 are shown in Figures 5.8 and 5.9. It is observed that the Ch-TGB transition is quite strong but relatively broad[21]. In contrast, the TGB-A transition in $X = 0.6$, is extremely weak, nevertheless clear on an enlarged scale (see inset of Figure 5.8). The A-C* transition is sharp and appears to be second order while the TGB-C* transition in $X = 0.66$, is quite strong. All these features are in good agreement with earlier observations[12,18,19].

5.3.3 X-ray diffraction studies

Layer spacing (d) measurements were carried out using samples filled in Lindemann glass capillaries and employing a computer controlled Guinier X-ray diffractometer (Huber 644). The temperature dependence of d for $X = 0.6$ is shown in Figure 5.10. On increasing the temperature d increases continuously in the C* phase, saturates in the A phase at a relatively constant value and continues to be so in the TGB phase. For $X = 0.66$ also (Figure 5.11), the d value increases with increasing temperature in the C* phase and attains a constant value in the TGB phase. The line profiles in the C*, A and TGB phases were found to be comparable but increase in width on going to the Ch phase. In both

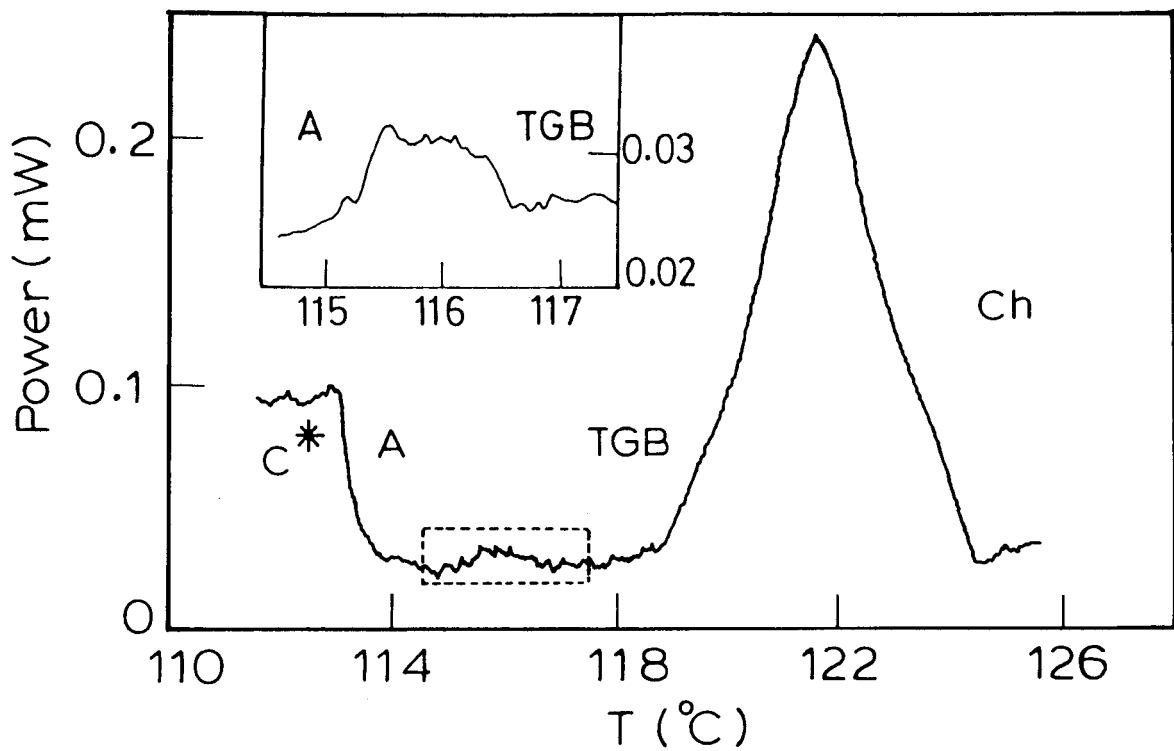


Figure 5.8: Differential scanning calorimeter scan obtained on heating (rate 5 °C/min) for $X = 0.6$. The region enclosed in dashed lines is shown on an enlarged scale as an inset.

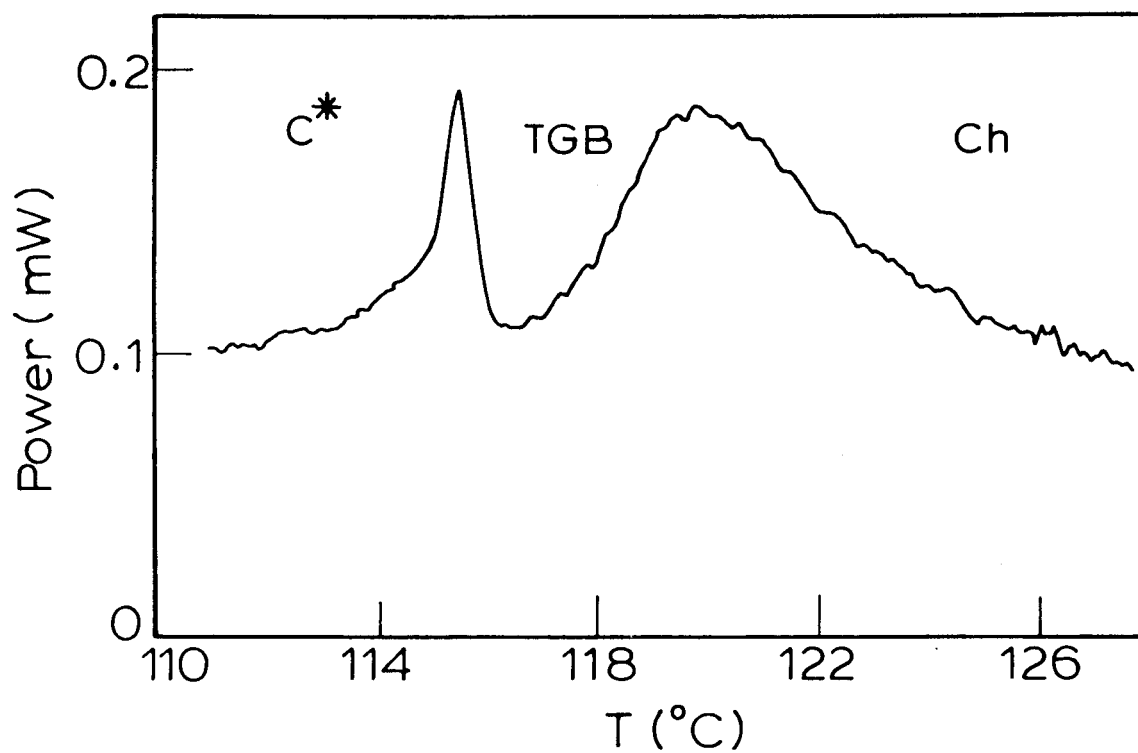


Figure 5.9: Differential scanning calorimeter scan obtained on heating (rate 5 °C/min) for $X = 0.66$.

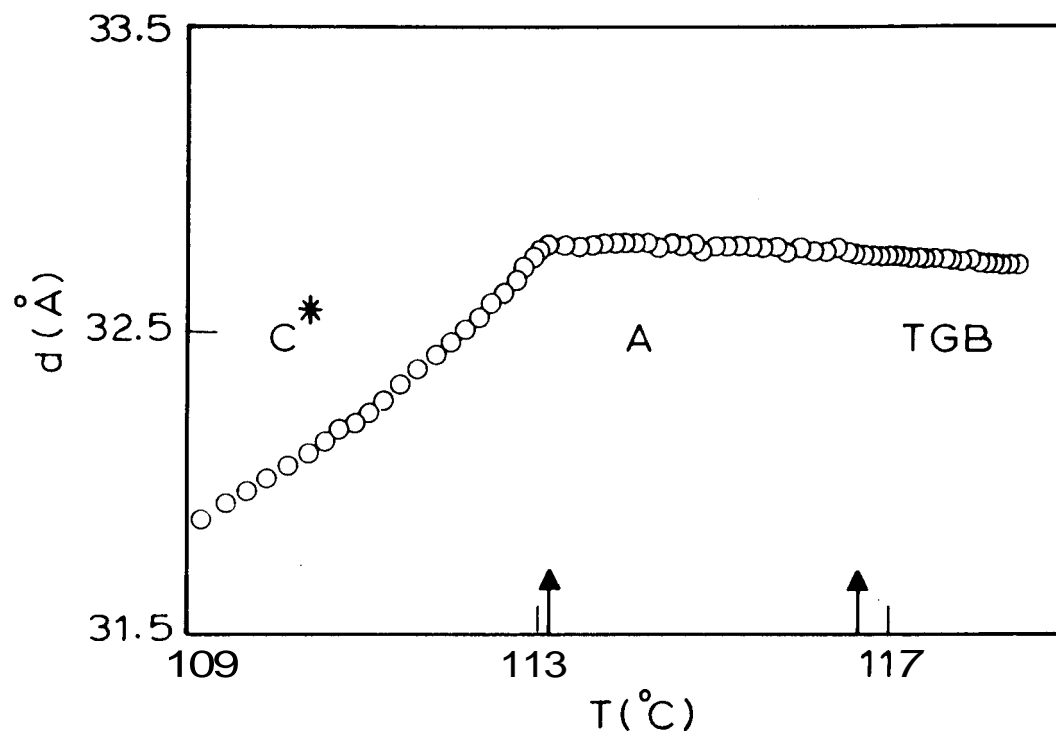


Figure 5.10: Temperature dependence of the smectic layer spacing for $X = 0.6$. The arrows indicate the C^* - A and A - TGB transition temperatures.

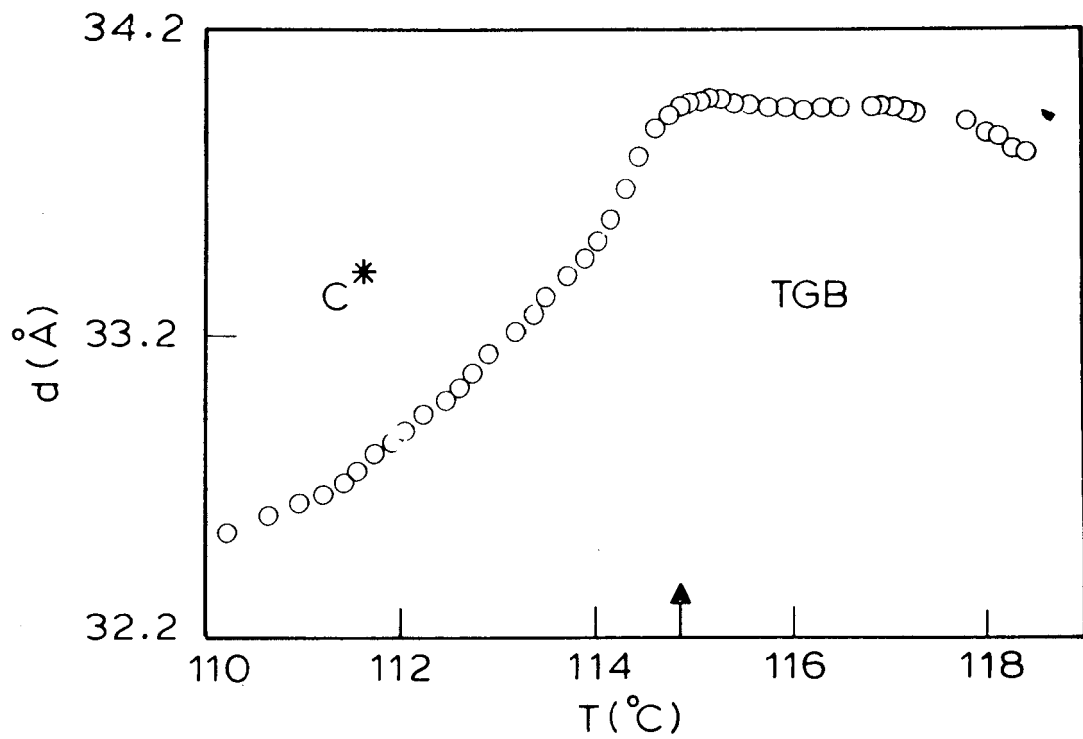


Figure 5.11: Temperature dependence of the smectic layer spacing for $X = 0.66$. The arrow indicates the C^* -TGB transition temperature.

A and TGB phases the d/l ratio (l = length of the molecule) was found to be ~ 0.9 , a value typical of a monolayer smectic A phase.

5.3.4 Selective reflection studies

A necessary feature of the TGB phase is the simultaneous existence of smectic layering as well as a macroscopic helical structure with its axis parallel to the layer planes. In order to demonstrate that the intermediate phase is indeed TGB, we have carried out transmitted light intensity measurements as a function of the incident beam wavelength. Experiments were done using a VIS/IR spectrophotometer (Hitachi U3400, wavelength range 400-2400 nm)[22]. Samples (thickness $\sim 50\mu\text{m}$) were contained between glass plates coated with a polymer solution and unidirectionally buffed, a procedure which produces an alignment of the molecular director parallel to the plates. This in turn aligns the helical axis of the TGB phase to be perpendicular to the glass surfaces. The sample cell was placed inside a calibrated hot stage whose temperature was regulated to a constancy of $\pm 25\text{ mK}$ during any scan. Optical transmission measurements were carried out at several temperatures in the Ch and TGB phases. The spectrum obtained for $X = 0.6$ at 1.1°C below the Ch-TGB transition is shown in Figure 5.12. The minimum observed at 2000 nm represents the wavelength λ_{min} of selective reflection from the TGB phase. The thermal variation of λ_{min} for two concentrations $X = 0.6$ and 0.66 are shown in Figure 5.13 and Figure 5.14. The trend observed (steady increase of λ_{min} as the temperature is lowered) and the value of the full width at half maximum of the spectra ($\sim 0.13 \lambda_{min}$) are in good agreement with the observations of Srajer et al[11] for the TGB phase of

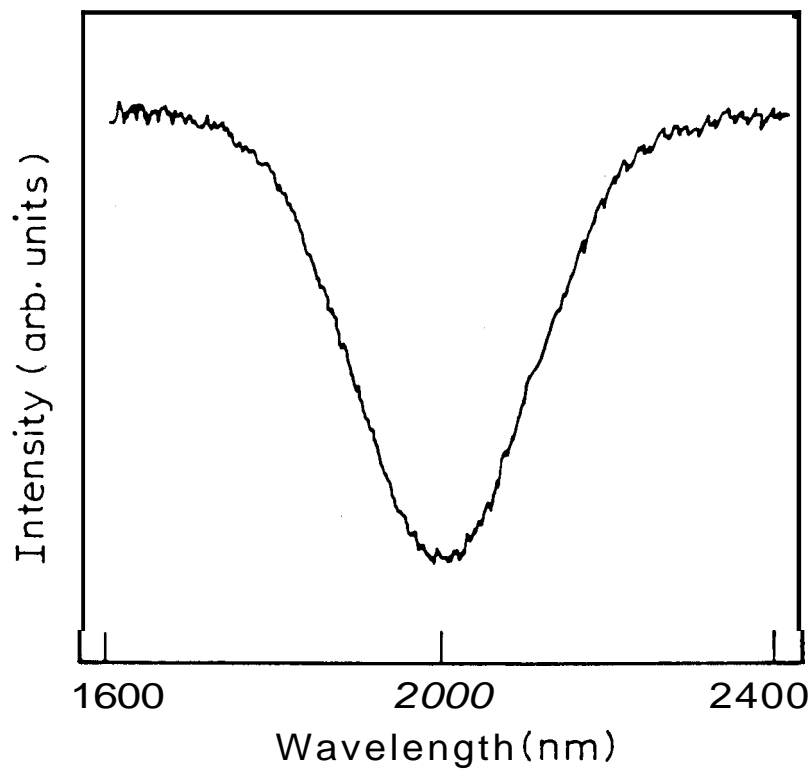


Figure 5.12: Typical optical transmission spectrum in the TGB phase for $X = 0.6$. The wavelength (λ_{min}) corresponding to the minimum in the plot is related to the pitch of the helical structure.

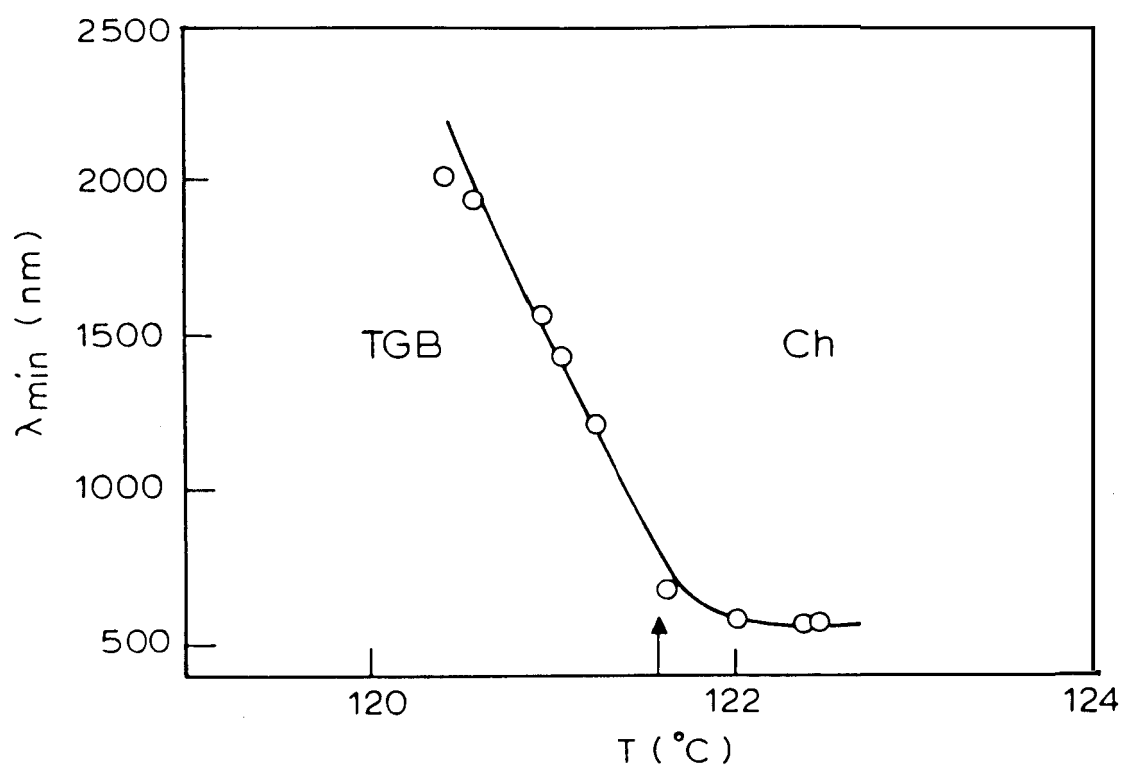


Figure 5.13: Temperature dependence of λ_{min} near the Ch-TGB transition for $X = 0.6$. The arrow indicates the transition temperature.

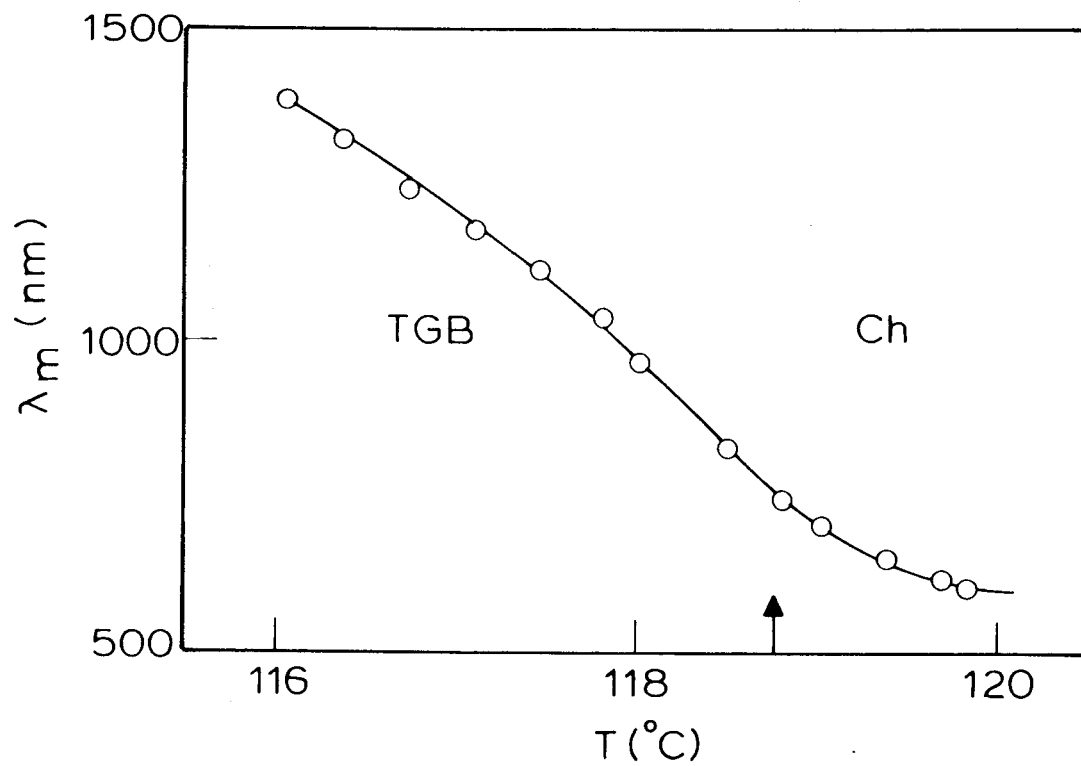


Figure 5.14: Temperature dependence of λ_{min} near the Ch-TGB transition for $X = 0.66$. The arrow indicates the transition temperature.

+14P1M7. These results, together with the X-ray and optical data presented above, confirm that this phase is the twist grain boundary phase.

All these results establish the existence of the TGB phase near a virtual chiral NAC point in a binary phase diagram as predicted by the theory.

References

- [1] D. L. Johnson, *J. Chim. Phys.* 80, 45 (1983).
- [2] D. Brisbin, D. L. Johnson, H. Fellner and M. E. Neubert, *Phys. Rev. Lett.* 50, 178 (1983); R. Shashidhar, B. R. Ratna and S. Krishna Prasad, *Phys. Rev. Lett.* 53, 2141 (1984).
- [3] S. R. Renn and T. C. Lubensky, *Phys. Rev. A* 38, 2132 (1988)
- [4] T. C. Lubensky and S. R. Renn, *Phys. Rev. A* 41, 4392 (1990).
- [5] S. R. Renn, *Phys. Rev. A* 45, 953 (1992).
- [6] J. H. Chen and T. C. Lubensky, *Phys. Rev. A* 14, 1202 (1976)
- [7] A. A. Abrikosov. *Sov. Phys. JETP* 5, 1174 (1957).
- [8] For a recent summary, see M. A. Anisimov, *Mol. Cryst. Liq. Cryst.* **162A**, 1 (1986).
- [9] D. S. Parmar, N. A. Clark, D. M. Walba and M. D. Wand, *Phys. Rev. Lett.* **62**, 213G (1989).
- [10] P. Pollmann and K. Schiulte, *Liquid Crystals* 10, 35 (1991)
- [11] G. Srajer, R. Pindak, M. A. Waugh, J. W. Goodby and J. S. Patel, *Phys. Rev. Lett.* 64, 1545 (1990).
- [12] J. W. Goodby, M. A. Waugh, S. M. Stein, E. Chin, R. Pindak and J. S. Patel, *Nature* 337, 449 (1989); *J. Am. Chem. Soc.* **111**, 8119 (1989).

- [13] P. G. de Gennes, *Solid State Commun.* 10, 753 (1972); W. L. McMillan as quoted by P.G.de Gennes in *Rev. Modern Phys.* 64, 645 (1992).
- [14] B. I. Halperin, T. C. Lubensky and S. K. Ma, *Phys. Rev. Lett.* 32, 292 (1974); J. H. Chen, T. C. Lubensky and D. R. Nelson, *Phys. Rev. B* 17, 4274 (1978).
- [15] C. Dasgupta and B. I. Halperin, *Phys. Rev. Lett.* 47, 1556 (1981); For a review see T. C. Lubensky, *J. Chim. Phys.* 80, 31 (1983).
- [16] C. W. Garland, M. Meichle, B. M. Ocko, A. R. Kortan, C. R. Safinya, L. J. Yu, J. D. Litster and R. J. Birgeneau, *Phys. Rev. A* 27, 3234 (1983); W.G.Bouman and W.H.de Jeu, *Phys. Rev. Lett.* 68, 800 (1992).
- [17] C. C. Huang, D. S. Lin, J. W. Goodby, M. A. Waugh, S. M. Stein and E. Chin, *Phys. Rev. A* 40, 4153 (1989).
- [18] O. D. Lavrentovich, Yu. A. Nastishin, V. I. Kulishov, Yu. S. Narkevich, A. S. Tolochko and S. V. Shiyanovskii, *Europhys. Lett.* 13, 313 (1990).
- [19] A. J. Slaney and J. W. Goodby, *J. Mater. Chem.* 1, 5 (1991).
- [20] J. W. Goodby and T. M. Leslie, *Mol. Cryst. Liq. Cryst.* 110, 175 (1984).
- [21] The transition temperatures for the TGB phase are often found to vary a little, particularly with respect to the method of examination. As the phase is essentially a frustrated phase it is possible that parameters like for example, surface pinning etc., can alter the transition temperatures and the actual temperature range of the phases involved.
- [22] The spectrometer was kindly provided by the Dept. of Inorganic and Physical Chemistry, I.I.Sc., Bangalore.